ISSN 2515-8260 Volume 09, Issue 04, 2022

Hydromagnetic Chemically Reacting and Radiating Casson Fluid Flow Past a Permeable Vertical Stretching Surface

Y. Hari Krishna[1]

[1]Dept of H&S, ANURAG Engineering College, Ananthagiri, Kodad, Telangana, India-508206

Abstract: In this article, we examine the concurrent impact of magnetic field, thermal radiation, buoyancy force, viscous dissipation and chemical reaction on Casson fluid flow, over a permeable stretching. The nonlinear model equations are obtained and transformed into a system of ordinary differential equations (ODE). Using shooting technique along with 6^{th} order Runge-Kutta iteration scheme, the model problem is tackled numerically. The effect of various embedded parameters on the velocity, temperature and concentration distributions are explained graphically while the skin friction coefficient, Nusselt number and Sherwood number are analysed and given in tabular form.

Keywords: Casson fluid, Prandtl number, bouncy parameter, Eckert number, Heat and Mass transfer

Introduction

In recent years, the study of Casson fluid flow, heat and mass transfer over a porous stretching surface in two-dimensional (2-D) boundary layers has brought considerable attention to this. These situations occur in processes in many industrial processes, such as polymer processing, paper production, food making, etc. We are particularly interested in all cases and non-Newtonian fluids are more suitable than Newtonian fluids. It is important to observe their behavior in order to know the characteristics of non-Newtonian fluid and their applications. Therefore, the researchers have been extremely interested in the boundary layer flows over the past few decades, which includes Casson fluid flow over a stretching surface that has different applications in the field of aerospace, medical, fiber producing.

Eldabe et al. [1] discussed Non-Newtonian Casson fluid flow between two rotating cylinders. Nadeem et al.[2] presented MHD flow of a Casson fluid over an exponentially shrinking sheet. Hayat et al. [3] have studied Soret and Dufour effects on magnetohydrodynamic (MHD) flow of Casson fluid. Pramanik [4] studied Casson fluid flow and heat transfer past an exponentially porous stretching surface. M. Gnaneswara Reddy [5] analysed Unsteady radiative-convective boundary layer flow of a Casson fluid with variable thermal conductivity. Khalid *et al.*[6] studied unsteady free convection flow of a Casson fluid. Akbar [7] depicts Influence of magnetic field on peristaltic flow of a Casson fluid. Khalid *et al.*[8] illustrated unsteady MHD free convection flow of Casson fluid. Raju *et al.*[9] studied Heat and mass transfer in magnetohydrodynamic Casson fluid. Bala [10] presented MHD flow of a Casson fluid over an exponentially inclined permeable stretching surface. Raju *et al.*[11] studied heat and mass transfer in MHD Casson fluid over an exponentially permeable stretching surface. Reddy *et al.* [12] discussed effects of joule heating on MHD free convective flow along a moving vertical plate. Reddy [13] studied Soret and Dufour effects on MHD free convective flow past a vertical porous plate. Mangathai *et al.*[14] illustrated MHD free convective flow past a vertical porous plate. Ramana *et al.*[15] discussed MHD mixed convection oscillatory flow over a vertical surface in a porous medium with chemical reaction and thermal radiation. Ramana Reddy *et al.*[16] studied Radiation and chemical reaction effects on MHD flow along a moving vertical porous plate. Very recently, the researchers [17-25] illustrated the heat and mass transfer behaviour of magnetohydrodynamic flows by considering stretching surface.

From the above studies, we say that little work has been made to analysis the Casson fluid flow considering thermal radiation and chemical reaction. The objective of the work is to study the Casson fluid flow and heat and mass transfer over a permeable vertical surface in presence of magnetic field , thermal radiation and chemical reaction effects numerically by

ISSN 2515-8260 Volume 09, Issue 04, 2022

shooting method. The effects of different involved parameter on the fluid velocity, temperature and concentration profiles along with friction factor coefficient, heat and mass transfer rates are discussed with help of graphs and tables.

Model Problem:

Consider a steady 2-D boundary layer flow of a viscous incompressible electrically conducting fluid along a permeable vertical stretching sheet with heat generation, thermal radiation and chemical reaction. Two equal and opposite forces are introduced along the x-axis so that the sheet is stretched keeping the origin fixed as seen in Figure 1. A magnetic field B_0 of uniform strength is applied in y-direction. The effect of the induced magnetic field is neglected in comparison to the applied magnetic field. Here x-axis is taken along the direction of the plate and y-axis normal to it.

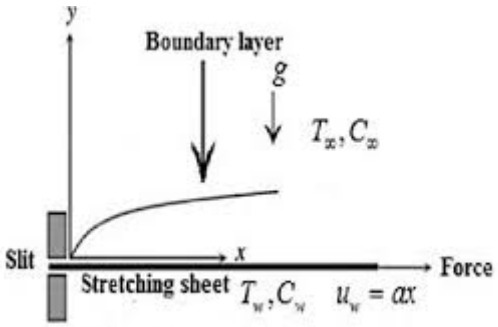

Then the equation of state for an isotropic flow of a Casson fluid is [1]

$$\tau_{ij} = 2\left(\mu_b + \frac{p_y}{\sqrt{2\pi}}\right)e_{ij} \tag{1}$$

where e_{ij} is the $(i,j)^{th}$ component of deformation rate, τ_{ij} is the $(i,j)^{th}$ component of the stress tensor, π is the product of the component of deformation rate with itself, and μ_b is the plastic dynamic viscosity. The yield stress P_y is expressed as, $P_y = \frac{\mu b\sqrt{2\pi}}{\beta}$ where β Casson fluid parameter. For non-Newtonian Casson fluid flow $\mu = \mu_b + \frac{P_y}{\sqrt{2\pi}}$ which gives $\nu' = \nu\left(1+\frac{1}{\beta}\right)$, where $\nu = \frac{\mu b}{\rho}$ is the kinematic viscosity for Casson fluid. It is assumed that plate temperature is initially T_W, while the temperature far away the sheet is T_∞. If u and v are the velocity components in x and y-directions respectively, then the governing equations for steady boundary layer flow of non-Newtonian Casson fluid are

$$\frac{\partial u}{\partial x} + \frac{\partial u}{\partial y} = 0 \tag{2}$$

$$u\frac{\partial u}{\partial x} + v\frac{\partial u}{\partial y} = \nu\left(1+\frac{1}{\beta}\right)\frac{\partial^2 u}{\partial y^2} + g_0\beta^*\left(T - T_\infty\right) - \frac{\sigma B_0^2}{\rho}u \tag{3}$$

$$u\frac{\partial T}{\partial x} + v\frac{\partial T}{\partial y} = \frac{k}{\rho c_p}\frac{\partial^2 T}{\partial y^2} + \frac{\nu}{c_p}\left(1+\frac{1}{\beta}\right)\left(\frac{\partial u}{\partial y}\right)^2 + \frac{\sigma B_0^2}{\rho c_p}u^2 + \frac{Q_0}{\rho c_p}\left(T - T_\infty\right) - \frac{1}{\rho c_p}\frac{\partial q_r}{\partial y}, \tag{4}$$

$$u\frac{\partial C}{\partial x} + v\frac{\partial C}{\partial y} = D_m\frac{\partial^2 C}{\partial y^2} - Kr\left(C - C_\infty\right) \tag{5}$$

where g_0 is the acceleration due to gravity, β^* is the volumetric co-efficient of thermal expansion, σ is the electric conductivity, B_0 is the uniform magnetic field strength, ρ is the

ISSN 2515-8260 Volume 09, Issue 04, 2022

fluid density, c_p is the specific heat at constant pressure, k is the thermal conductivity, Q_0 is the volumetric rate of heat generation and q_r is the radiative heat flux. Dm is the coefficient of the mass diffusivity, C is the concentration of the fluid, Kr is the chemical reaction parameter,

The corresponding boundary conditions are

$$\left.\begin{array}{ll} u = u_w, v = v_w(x), & T = T_w, C = C_w \quad at\ y = 0 \\ u = 0, & T = T_\infty,\ C = C_\infty \quad as\ y \to \infty \end{array}\right\} \tag{6}$$

where $u_w\ uw$ is the tangential velocity and we consider $u_w = Dx, D(>0)$ is a constant and v_w is the suction velocity.

Using Rosseland approximation for radiation we can get

$$q_r = -\frac{4\sigma^*}{3k'}\frac{\partial T^4}{\partial y} \tag{7}$$

where σ^* is the Stefan- Boltzman constant and $3k'$ is the absorption coefficient. Here we consider the temperature difference within the flow is very small such that T^4 may be expanded as a linear function of temperature. Using Taylor series and neglecting the higher order terms, we get, $T^4 \cong 4T_\infty^3 T - 3T_\infty^4$. Thus equation (4) implies

$$u\frac{\partial T}{\partial x} + v\frac{\partial T}{\partial y} = \frac{k}{\rho c_p}\frac{\partial^2 T}{\partial y^2} + \frac{\upsilon}{c_p}\left(1+\frac{1}{\beta}\right)\left(\frac{\partial u}{\partial y}\right)^2 + \frac{\sigma B_0^2}{\rho c_p}u^2 + \frac{Q_0}{\rho c_p}(T - T_\infty) + \frac{16\sigma^* T_\infty^3}{3k'\rho c_p}\frac{\partial^2 T}{\partial y^2} \tag{8}$$

The governing equations (3) and (8) can be made dimensionless by introducing the following similarity variables.

$$u = Dxf'(\eta), v = -\sqrt{D\vartheta}\,f(\eta) = y\sqrt{\frac{D}{\vartheta}}, \psi = \sqrt{D\vartheta}xf(\eta), \theta(\eta) = \frac{T - T_\infty}{T_w - T_\infty}, \phi(\eta) = \frac{C - C_\infty}{C_w - C_\infty} \tag{9}$$

where ψ is the stream function, η is the dimensionless distance normal to the sheet, θ be the dimensionless temperature, ϕ be the dimensionless concentration

Using equation (9) in equations (3) and (8), we get

$$\left(1+\frac{1}{\beta}\right)f''' + ff'' - f'^2 + \gamma\theta - Mf' = 0 \tag{10}$$

$$\left(1+\frac{4}{3}N\right)\theta'' + \Pr\, f\theta' + \left(1+\frac{1}{\beta}\right)Ec\,\Pr(f'')^2 + MEc\,\Pr(f')^2 + \Pr Q\theta = 0, \tag{11}$$

$$\phi'' + NSc(4f'\phi - f\phi') - ScKr\phi = 0 \tag{12}$$

The reduced boundary conditions are

$$\left.\begin{array}{lll} f' = 1, & f = f_w, & \theta = 1, \phi = 1 \quad at\ \eta = 0 \\ f' = 0, & & \theta = 0, \phi = 0 \quad as\ \eta \to \infty \end{array}\right\} \tag{13}$$

where $M = \frac{\sigma B_0^2}{\rho D}$ is the magnetic field parameter, $\gamma = \frac{go\beta_T(T_w - T_\infty)}{D^2 x}$ is the buoyancy parameter, $Q = \frac{Q_0}{D\rho c_p}$ is the heat source parameter, $\Pr = \frac{\mu c_p}{k}$ is the Prandtl number, $Ec = \frac{D^2 x^2}{c_p(T_w - T_\infty)}$ is the Eckert number, $f_w = -\frac{v_w}{\sqrt{D\vartheta}}$ is the suction parameter and $N = \frac{4\sigma^* T_\infty^3}{kk'}$ is the radiation parameter. $Sc = \frac{\nu_f}{D_m}$ is the Schmidt number, $Kr = \frac{K_0 L}{C_0 U_0}$ is the chemical reaction

ISSN 2515-8260 Volume 09, Issue 04, 2022

Finally, skin friction coefficient$\left(C_f\right)$, local Nusselt number $\left(Nu_x\right)$ and Sherwood number $\left(\mathrm{Re}_x\right)$ can be written as

$$C_f \,\mathrm{Re}_x^{1/2} = \left(1+\frac{1}{\beta}\right) f''(0),\ Nu_x \,\mathrm{Re}_x^{-1/2} = -\left(1+\frac{4}{3}N\right)\theta'(0),\ Sh_x \,\mathrm{Re}_x^{-1/2} = -\phi'(0) \qquad (14)$$

Numerical Procedure

The system non-linear differential equations (10)-(12) with the boundary conditions (13) have been solved numerically by shooting technique along with 6thorder Runge-Kutta iteration scheme with MATLAB package. The step size $\Delta\eta$ = 0.01 is chosen to satisfy the convergence criterion of 10^{-6} in all cases. The value of η_∞ was found to each iteration loop by $\eta_\infty = \eta_\infty + \Delta\eta$. The maximum value of η_∞ to each group of parameters β, fw, Q,M, Pr,Ec and N determined when the value of the unknown boundary conditions at $\eta = 0$ not change to successful loop with error less than 10^{-6}.

Results and Discussion

The results are showing the nature of the effects of the parameters like β, γ, M,N,Pr, Q,Sc,Ec and Kr are Casson parameter, Bouncy parameter, Magnetic parameter, thermal radiation parameter, Prandtl number, Heat source parameter, Schmidt number, Eckert number and chemical reaction parameter respectively, on velocity and temperature and concentration profiles are displayed with help of graphical illustration. Also the friction factor, Nusselt number and Sherwood number are discussed and given in tabular form. For numerical results used β=1; γ=1; M=0.5; N=0.2; Pr=0.71; Q=0.5; Sc=0.6; Kr=0.5; w=0.5;Ec=0.1, these are values are treated as common throughout the study expert the varied values in respective figures and table.

Figure 2 show the plot of the effect of Casson parameter on velocity profile. It is observed that the velocity decreases when Casson increases. In practice, increasing results in an increase in the plastic dynamic viscosity that produces a resistance in the flow and decrease in fluid velocity thereof. In Figure 3, velocity boundary layer thickness increases with increasing values of Bouncy parameter$\left(\gamma\right)$. The thermal buoyancy parameter $\left(\gamma\right)$ effect on the concentration is revealed using figure 4. It is found that an increase of the thermal buoyancy parameter $\left(\gamma\right)$ increases the thermal conductivity of the fluid. Figure 5 depicts the depreciation of velocity for higher intensities of the M. this is in conformity with the fact that stronger Lorentz force, generated as a result of higher magnetic field strength, heavily opposes the fluid motion. Figure 6 depicts that when the magnetic field parameter M increases the temperature distribution of the fluid increases. It is because the existence of the magnetic field creates a Lorentz force that opposes the motion of a fluid and increases the thermal conductivity of the fluid. In Figure 7, the effect of an applied magnetic field is found to increase the concentration boundary layer. However, it is interesting to note that the concentration profiles decrease with the increase of both heat source and chemical reaction parameters. Figures 8-10 represents the effect of the Prandtl number (Pr) on the velocity, temperature and concentration profiles of the flow field. It is observed that the Pr has no significant impact on the concentration profiles of the flow shown in Figure 9 and 10, but temperature and concentration profiles of the flow decreases as the Pr increases. Temperature and thermal boundary layer thickness are decreased the corresponding to an increase in the values of Pr. Fig 8 reveals the effects of Pr on the transient velocity profiles. It is evident

ISSN 2515-8260 Volume 09, Issue 04, 2022

form the figure that the velocity decreases with an increase in Pr. Figure 11 shows that velocity increases as heat source parameter Q increases. In Figure (12) we have illustrated non-dimensional temperature profiles against η for some representative values of the heat source parameter Q = 0.2, 0.5, 0.7,0.9. The positive value of Q represents source i.e. heat generation in the fluid. We know that when heat is generated the buoyancy force increases, which induces the flow rate to increase, giving rise to increase in the temperature profiles. Figure 13 shows that concentration increases as heat source parameter Q increases. The effect of the Schmidt number Sc on the flow profiles is shown in Fig 14. It can be seen from the figure that, as the Sc increases, the flow concentration decrease across the boundary layer region, a higher Sc implies a lower Brownian diffusion coefficient, which will give rise to a shorter penetration depth for concentration boundary layer. Figure 15 illustrates the influence of the non-dimensional chemical reaction parameter (Kr) on the concentration profile flow. The effect of the Kr is very important in the concentration field. It can infer from Fig13 that concentration profiles of the fluid decrease with increasing values of the Kr. This is because of in Kr speed up the rate of the reactants on the flow and consequently reduces the concentration distribution of the reacting species. Figure 16 and 17 depicts the effect of varying thermal radiation parameter N on the flow temperature and concentration flow. The temperature distribution is enhanced with an increase in the N. Large values of N provide more heat to working fluid, which results in an enticement in the temp and thermal boundary layer thickness. Effect of N on the concentration, we observed that increase values of N concentration increases. Figure 18 depicts dimensionless temperature and temperature gradient for various values of Eckert number Ec, although an increase in the temperature profiles, as well as the thickness of the boundary layer, is observed with an increase in the Eckert number, it yields a decrease in the rate of heat transfer. Thus, by varying the Eckert number, the wall temperature distribution can be manipulated.

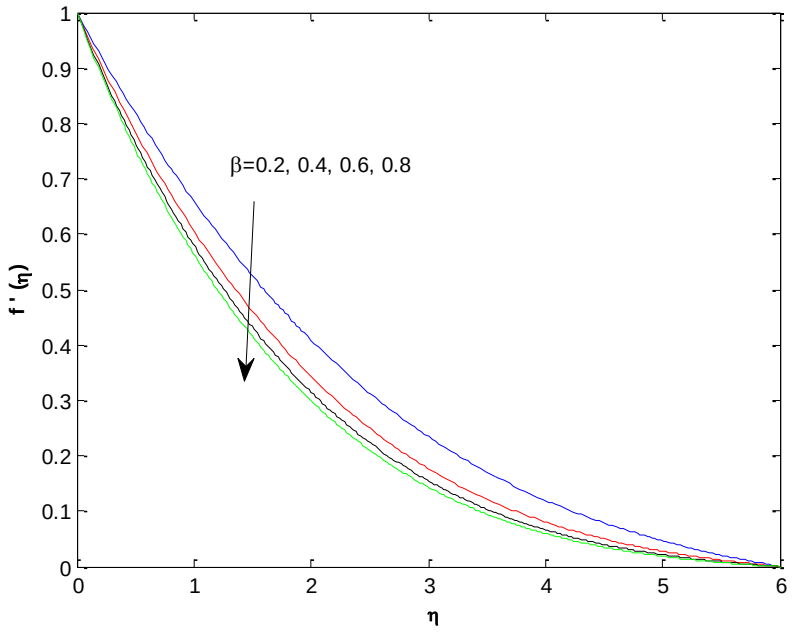

Figure 2: Dominance of β on Velocity

ISSN 2515-8260 Volume 09, Issue 04, 2022

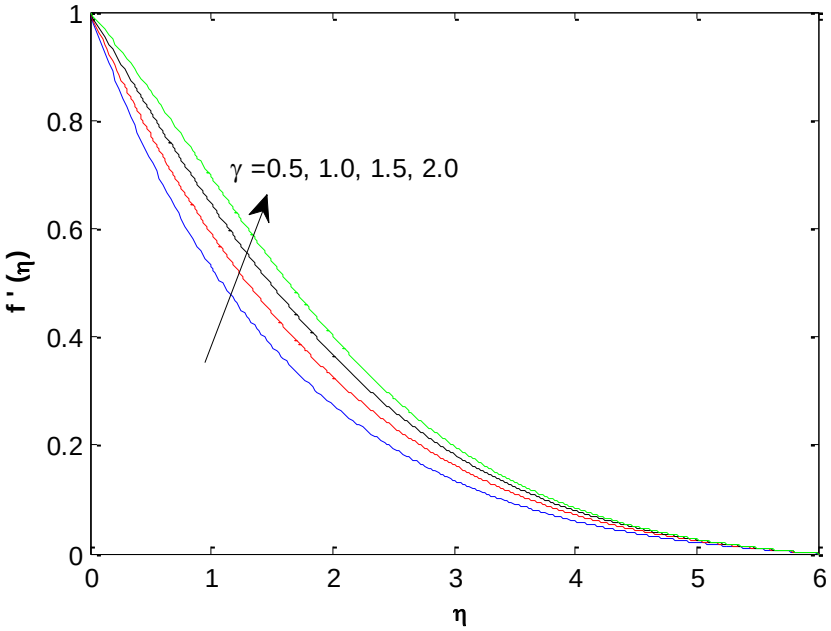

Figure 3: Dominance of γ on Velocity

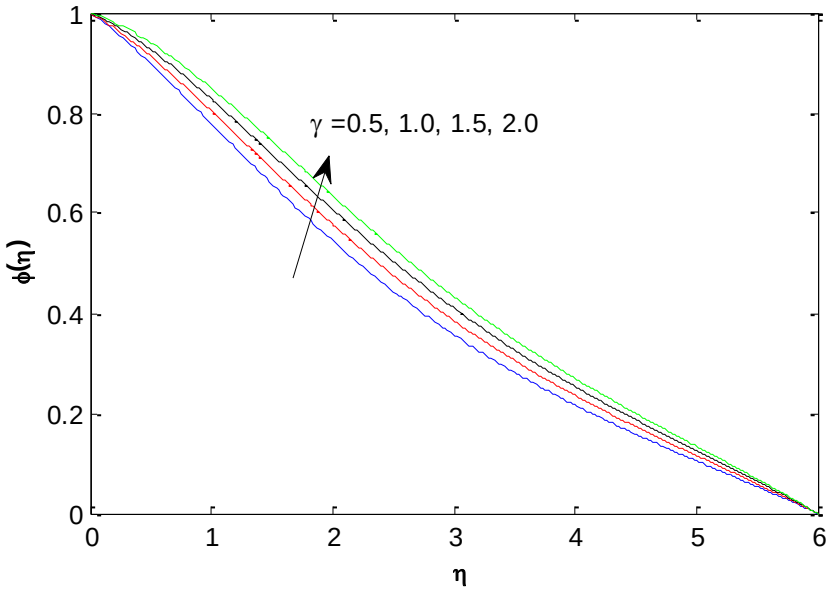

Figure 4: Dominance of γ on Concentration

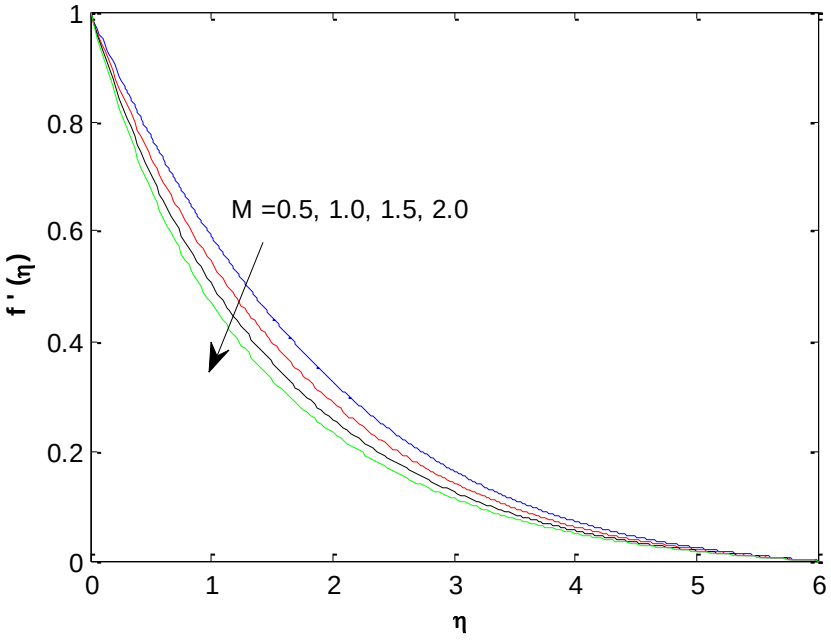

Figure 5: Dominance of M on Velocity

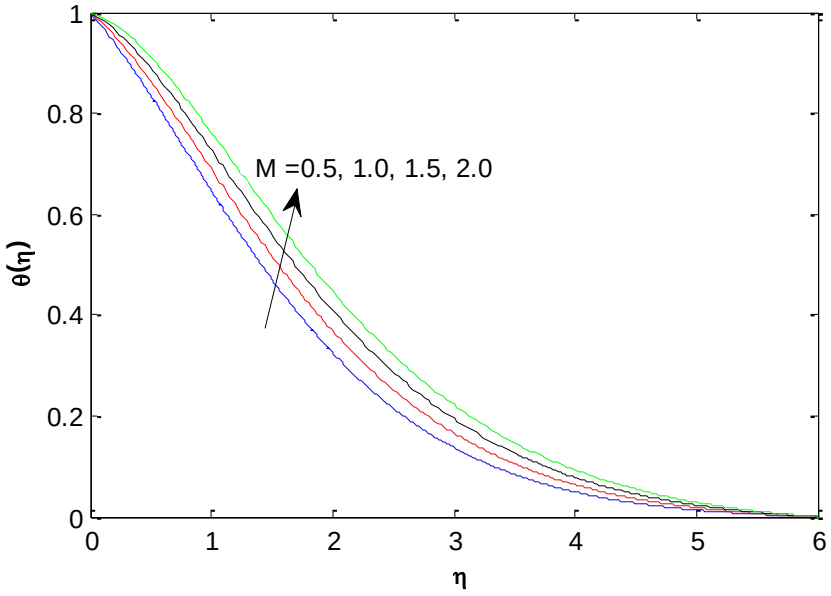

Figure 6: Dominance of M on Temperature

ISSN 2515-8260 Volume 09, Issue 04, 2022

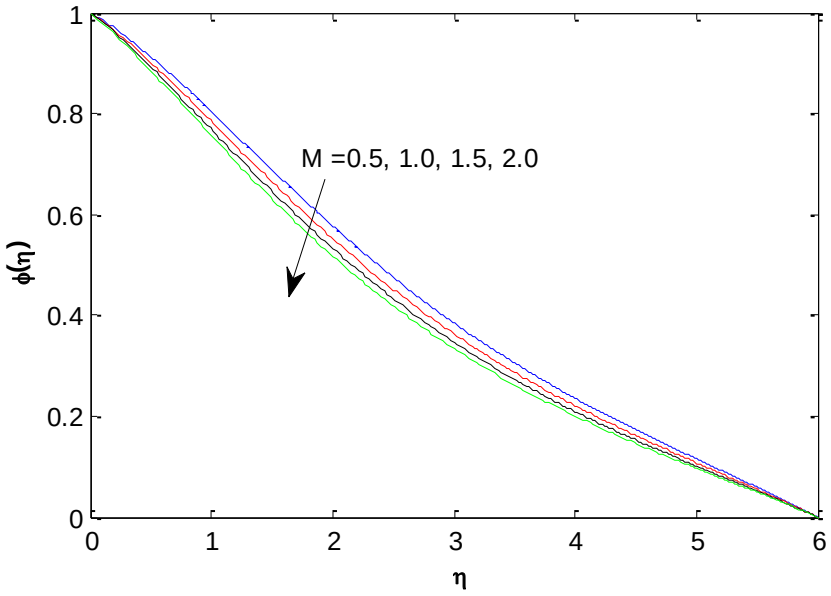

Figure 7: Dominance of M on Concentration

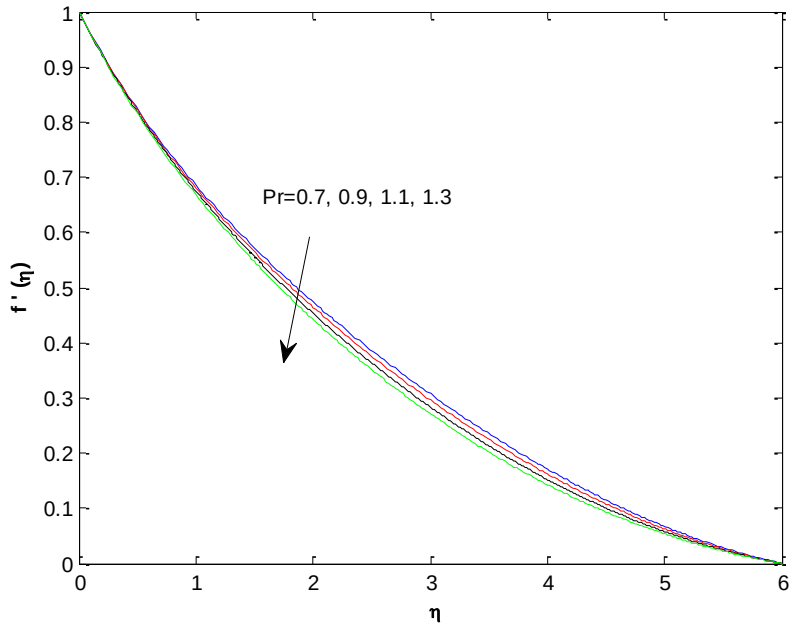

Figure 8: Dominance of Pr on Velocity

ISSN 2515-8260 Volume 09, Issue 04, 2022

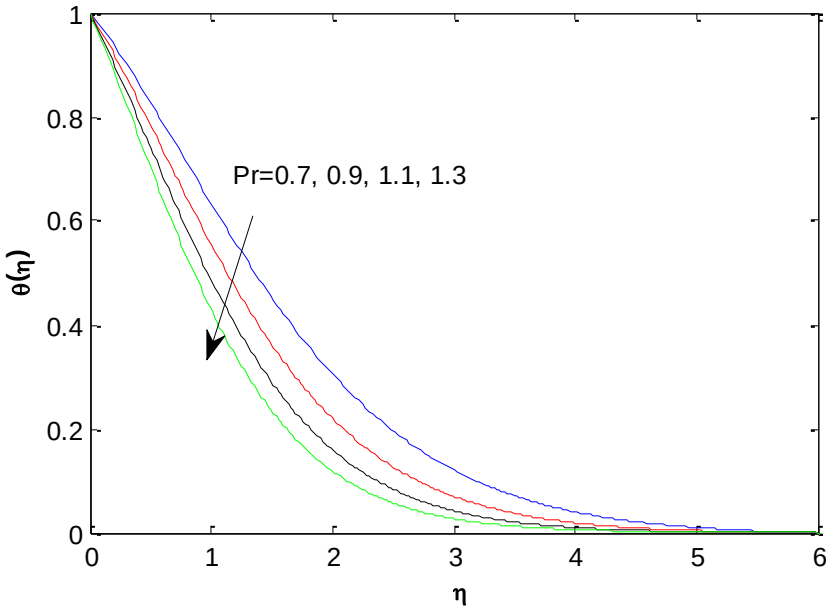

Figure 9: Dominance of Pr on Temperature

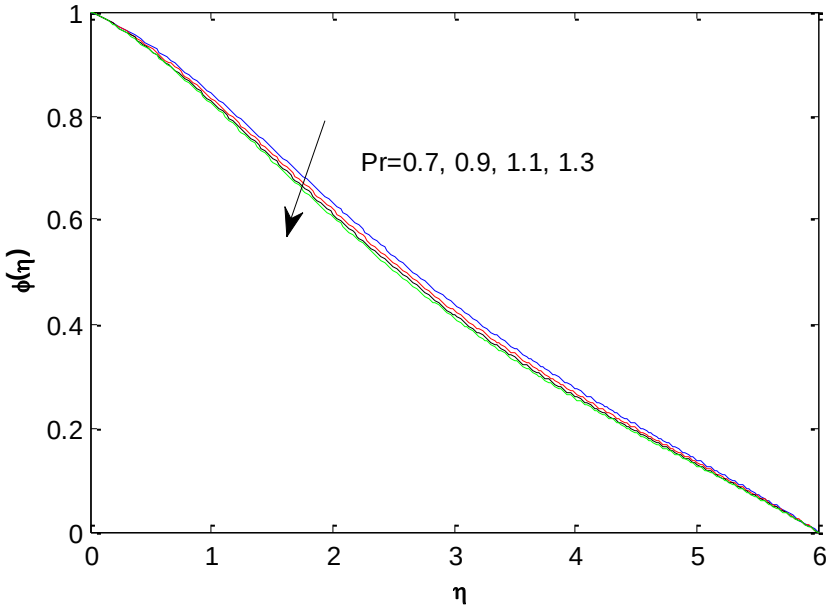

Figure 10: Dominance of Pr on Concentration

ISSN 2515-8260 Volume 09, Issue 04, 2022

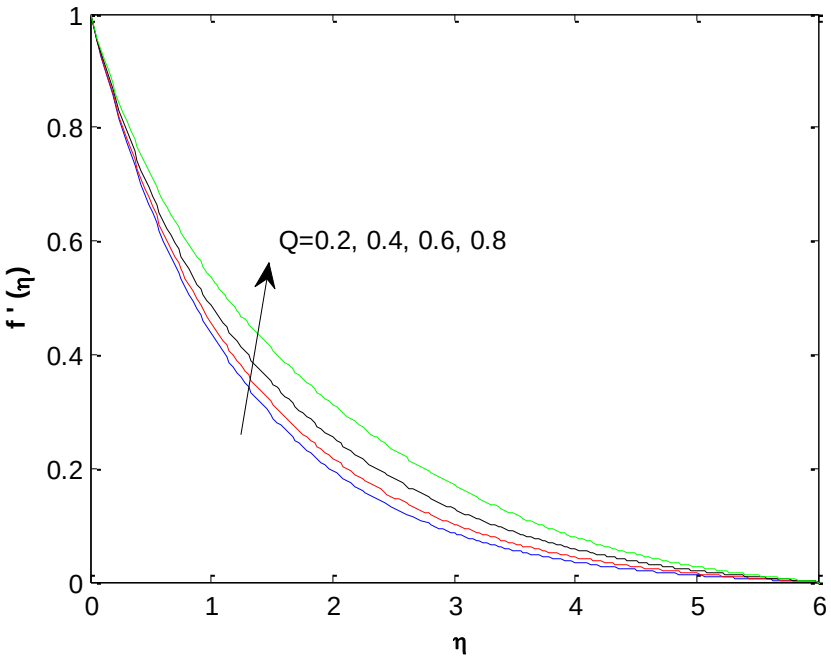

Figure 11: Dominance of Q on Velocity

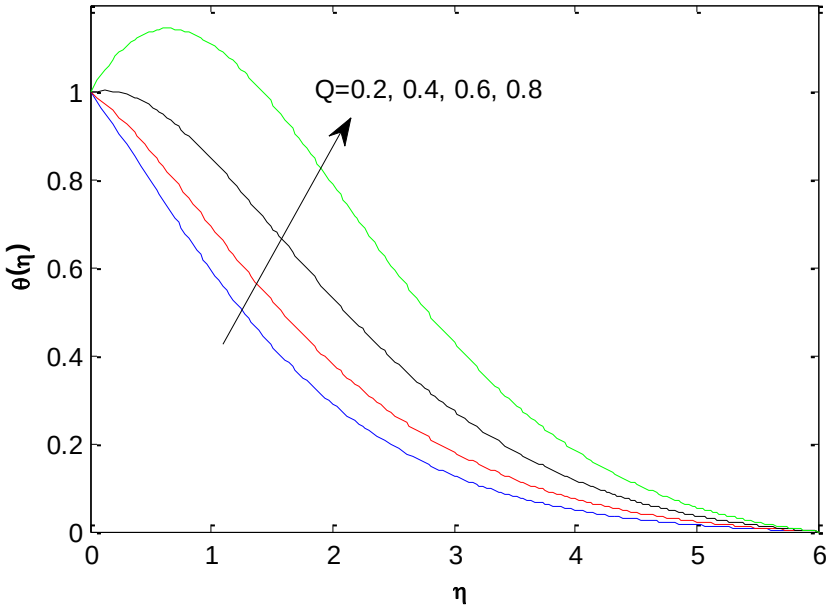

Figure 12: Dominance of Q on Temperature

ISSN 2515-8260 Volume 09, Issue 04, 2022

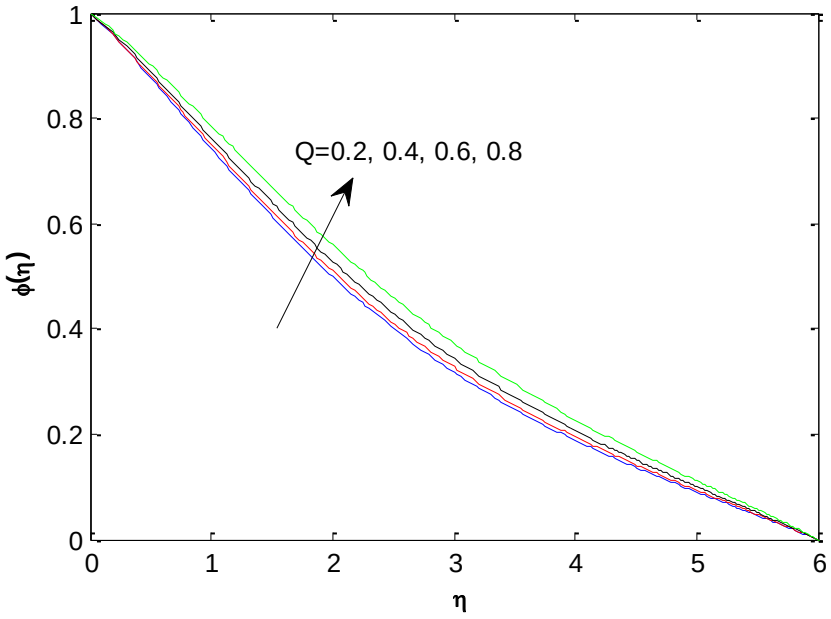

Figure 13: Dominance of Q on Concentration

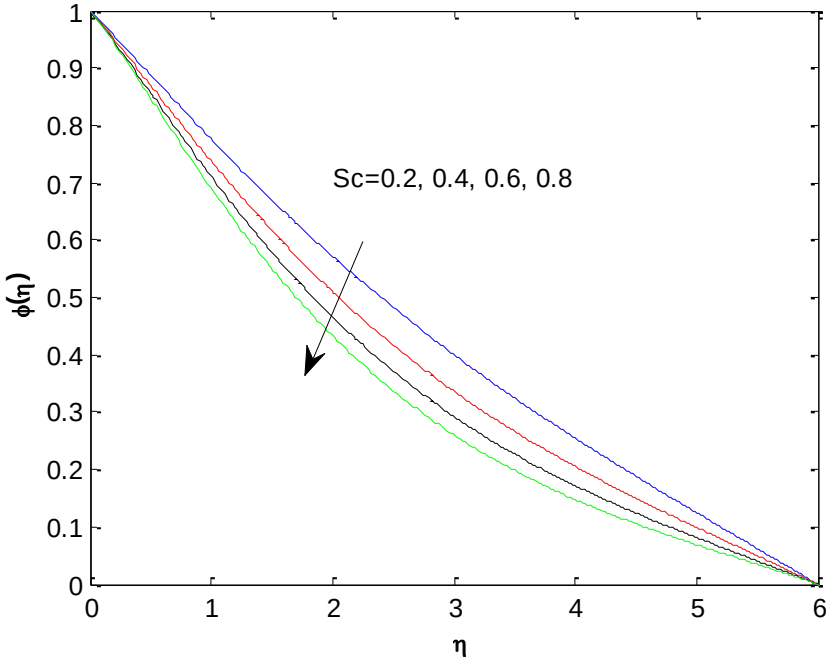

Figure 14: Dominance of Sc on Concentration

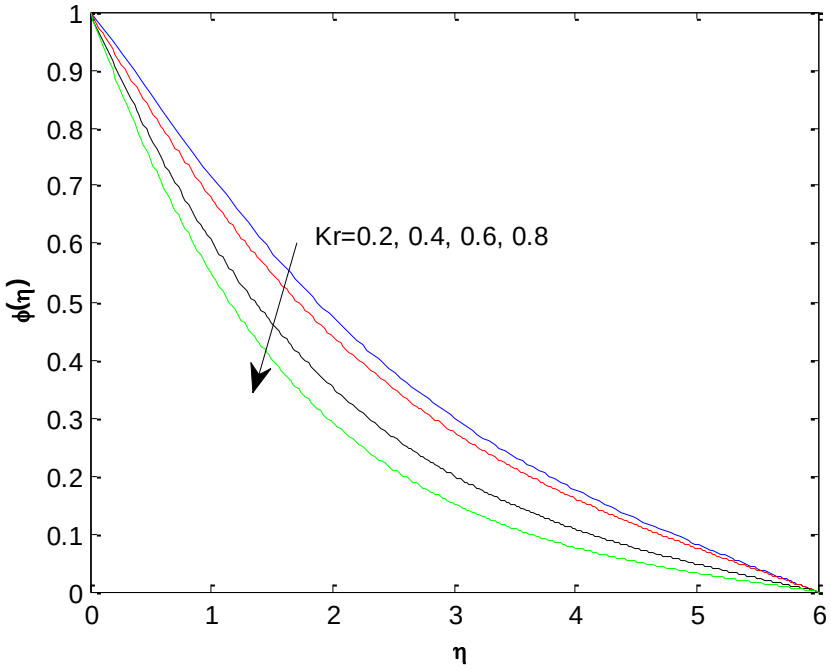

Figure 15: Dominance of Kr on Concentration

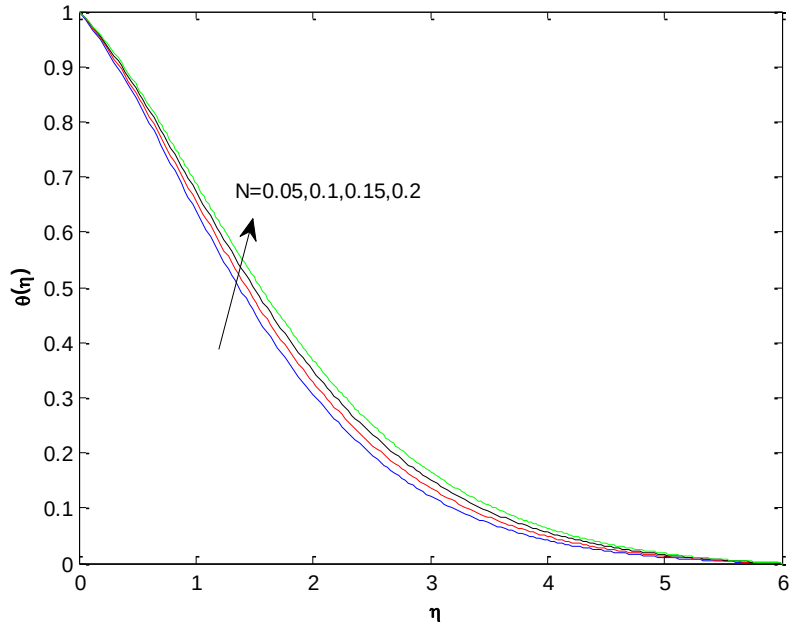

Figure 16: Dominance of N on Temperature

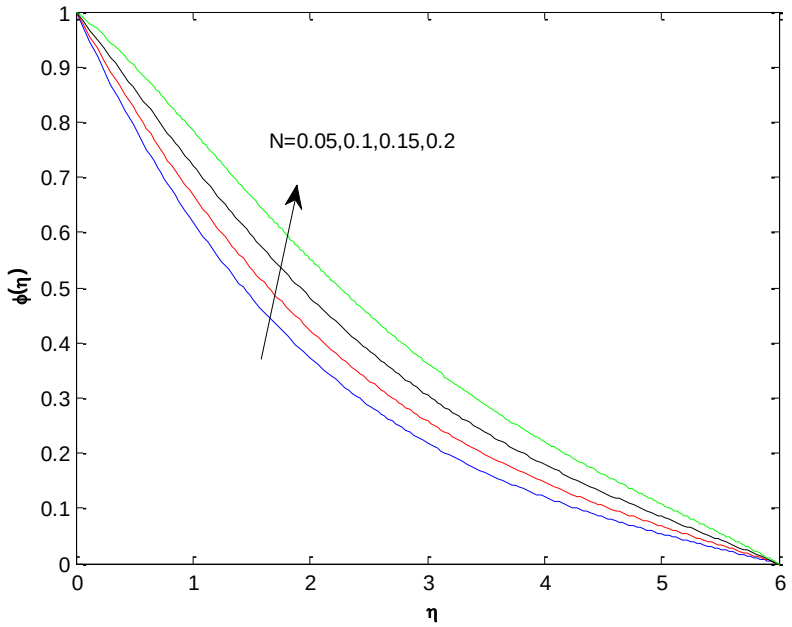

Figure 17: Dominance of N on Concentration

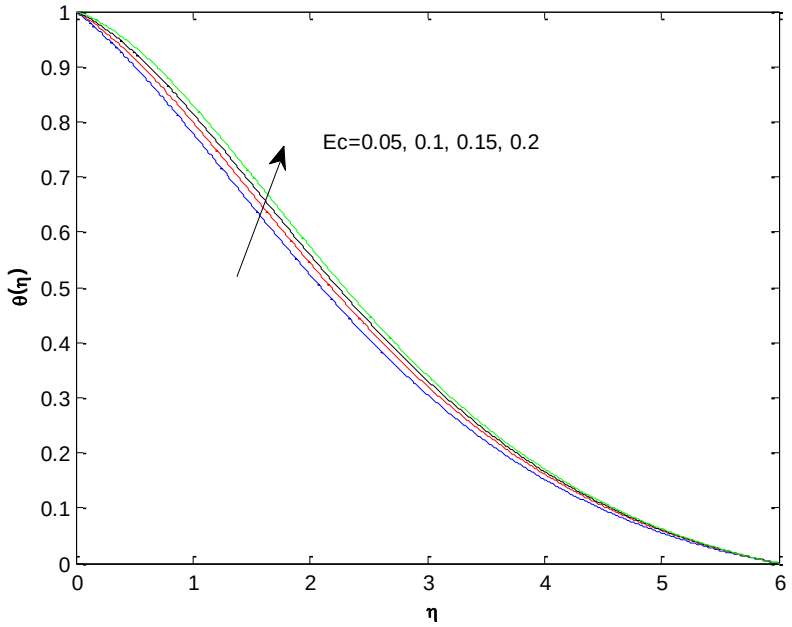

Figure 18: Dominance of Ec on Temperature

Conclusion:

This study presented the flow, heat and mass transfer behaviour of Casson fluid over a permeable vertical stretching surface considering the effects of magnetic field and thermal radiation and chemical reaction. The conclusions are as follows:

1. Velocity decreases for increasing values of Casson parameter, magnetic parameter M, Prandtl number Pr where as it shows reverse tendency in the case of bouncy parameter (γ) and heat Source parameter Q.
2. Temperature distribution decreases with an increase in Prandtl number Pr where as it shows reverse tendency in the case of and heat Source parameter Q, thermal radiation parameter N, magnetic parameter M and Eckert number Ec.
3. Concentration boundary layer decreases with an increase in Prandtl number Pr, chemical reaction Kr, magnetic parameter M and Schmidt number Sc where as it shows reverse

ISSN 2515-8260 Volume 09, Issue 04, 2022

tendency in the case of thermal radiation parameter N, heat Source parameter Q and bouncy parameter (γ).

References:

1. Eldabe, N. T. M., Saddeck, G. & El-Sayed, A. F. [2001] "Heat transfer of MHD non-Newtonian Casson fluid flow between two rotating cylinders", Mechanics and Mechanical Engineering, Vol. 5, Issue. 2, pp. 237-251.
2. Nadeem, S., Haq, R. U., & Lee, C.[2012] "MHD flow of a Casson fluid over an exponentially shrinking sheet," Scientia Iranica, Vol. 19, Issue. 6, pp.1550-1553.
3. T. Hayat, S.A. Shehzad, A. Alsaedi, Soret and Dufour effects on magnetohydrodynamic (MHD) flow of Casson fluid, Appl. Math. Mech. 33 (10) (2012) 1301–1312.
4. S.Pramanik, Casson fluid flow and heat transfer past an exponentially porous stretching surface in presence of thermal radiation, Ain Shams Engineering Journal, Volume 5, Issue 1, March 2014, Pages 205-212
5. M. Gnaneswara Reddy, Unsteady radiative-convective boundary layer flow of a Casson fluid with variable thermal conductivity, J. Eng. Phys. Thermo Phys. 88 (1) (2015) 240–251.
6. A. Khalid, I. Khan, S. Shafiel, Exact solutions for unsteady free convection flow of a Casson fluid over an oscillating vertical plate with constant wall temperature, Abstr. Appl. Anal. (15) (2015) 946350 <http://dx.doi.org/10.1155/2015/946350>.
7. N. Akbar, Influence of magnetic field on peristaltic flow of a Casson fluid in an asymmetric channel: application in crude oil refinement, J. Magnet. Magnet. Mater. 378 (2015) 463–468.
8. A. Khalid, I. Khan, A. Khan, S. Shafie, Unsteady MHD free convection flow of Casson fluid past over an oscillating vertical plate embedded in a porous medium, Eng. Sci. Technol. Int. J. (2015) doi:10.1016/j.jestch.2014.12.006.
9. C.S.K. Raju, N. Sandeep , V. Sugunamma, M. Jayachandra Babu, J.V. Ramana Reddy, Heat and mass transfer in magnetohydrodynamic Casson fluid over an exponentially permeable stretching surface, Engineering Science and Technology, an International Journal 19(2016), 45-52
10. P. BalaAnkiReddy, Magnetohydrodynamic flow of a Casson fluid over an exponentially inclined permeable stretching surface with thermal radiation and chemical reaction Ain Shams Engineering Journal Volume 7, Issue 2, June 2016, Pages 593-602
11. Raju, C. S. K., Sandeep, N., Sugunamma, V., Babu, M. J., & Reddy, J. R. [2016] "Heat and mass transfer in magnetohydrodynamic Casson fluid over an exponentially permeable stretching surface", Engineering Science and Technology, an International Journal, Vol. 19, Issue. 1, pp. 45-52.
12. Reddy, R. C., Reddy, K. J., & Ramakrishna, K. (2016). Effects of joule heating on MHD free convective flow along a moving vertical plate in porous medium. Special Topics and Reviews in Porous Media, 7(2), 207-219. doi:10.1615/SpecialTopicsRevPorousMedia.2016017247
13. Reddy, G. V. R. (2016). Soret and Dufour effects on MHD free convective flow past a vertical porous plate in the presence of heat generation. International Journal of Applied Mechanics and Engineering, 21(3), 649-665. doi:10.1515/ijame-2016-0039
14. Mangathai, P., Ramana Reddy, G. V., & Rami Reddy, B. (2016). MHD free convective flow past a vertical porous plate in the presence of radiation and heat generation. International Journal of Chemical Sciences, 14(3), 1577-1597.

ISSN 2515-8260 Volume 09, Issue 04, 2022

15. Ramana Reddy, G. V., Bhaskar Reddy, N., & Chamkha, A. J. (2016). MHD mixed convection oscillatory flow over a vertical surface in a porous medium with chemical reaction and thermal radiation. Journal of Applied Fluid Mechanics, 9(3), 1221-1229.
16. Ramana Reddy, G. V., Bhaskar Reddy, N., & Gorla, R. S. R. (2016). Radiation and chemical reaction effects on MHD flow along a moving vertical porous plate. International Journal of Applied Mechanics and Engineering, 21(1), 157-168. doi:10.1515/ijame-2016-0010
17. P.Suresh, Y. Hari Krishna, R. Sreedhar Rao, P. V. Janardhana Reddy; "Effect of Chemical Reaction and Radiation on MHD Flow along a moving Vertical Porous Plate with Heat Source and Suction", International Journal of Applied Engineering Research, 14(4), 869-876, 2019
18. BalajiPrakash, G; Reddy, GV Ramana; Sridhar, W; Krishna, Y Hari; Mahaboob, B; Thermal Radiation and Heat Source Effects on MHD Casson Fluid over an Oscillating Vertical Porous Plate, Journal of Computer and Mathematical Sciences,10(5),1021-1031,2019
19. P.Suresh, Y. Hari Krishna, Mahaboob, Amaranath: Heat Transfer and Stagnation Heat Stagnation-Point Flow of Non-Point Non-Newtonian Casson Fluid over Stretching Surface Fluid Surface, International Journal of Modern Engineering and Research Technology, Volume 6 | Issue 2 | April 2019,33-39
20. N Vijaya, Y Hari Krishna, K Kalyani, GVR Reddy Non-Aligned Stagnation Point Flow of a Casson Fluid past a Stretching Sheet in a Doubly Stratified Medium, « Fluid Dynamics & Materials Processing, vol.15, no.3, pp.233-251, 2019
21. M M Hasan. "Casson Fluid Flow and Heat Transfer over a Permeable Vertical Stretching Surface with Magnetic Field and Thermal Radiation." IOSR Journal of Engineering (IOSRJEN), vol. 09, no. 01, 2019, pp. 14-19.
22. S. Y. Ibrahim and O. D. Makinde, "Radiation effect on chemically reacting magnetohydrodynamics (MHD) boundary layer flow of heat and mass transfer through a porous vertical flat plate," International Journal of Physical Sciences, vol. 6, no. 6, pp. 1508–1516, 2011.
23. O. D. Makinde, "Free convection flow with thermal radiation and mass transfer past a moving vertical porous plate," International Communications in Heat and Mass Transfer, vol. 32, no. 10, pp. 1411–1419, 2005.
24. O. D. Makinde and A. Ogulu, "The effect of thermal radiation on the heat and mass transfer flow of a variable viscosity fluid past a vertical porous plate permeated by a transverse magnetic field," Chemical Engineering Communications, vol. 195, no. 12, pp. 1575–1584, 2008.
25. C. Sulochana, S.P. Samrat, N. Sandeep Numerical investigation of magnetohydrodynamic (MHD) radiative flow over a rotating cone in the presence of Soret and chemical reaction, Propulsion and Power Research, Volume 7, Issue 1, 2018, pp. 91-101